Journal of Communicable Diseases
Volume 57, Issue 2 - 2025, Pg. No. 19-31
Peer Reviewed & Open Access Journal

Research Article

Anti-enzymatic Activity of Alhagi Maurorum Extract and Copper oxide Nanoparticles against *Acinetobacter Baumannii* Respiratory Infection

Marwa Amin Al-Rawi[1], Bareq N Al-Nuaimi[2], Nada H A Al-Mudallal[3], Mohammed Ameen Ahmed Al-Rawi[4]

[1]Assistant Lecturer, [2]Lecturer, [3]Professor, Department of Microbiology, College of Medicine, Al-Iraqia University, Baghdad, Iraq
[4]Neurosurgeon, Neurosurgery Teaching Hospital, Baghdad, Iraq
DOI: https://doi.org/10.24321/0019.5138.202533

I N F O

Corresponding Author:
Bareq N Al-Nuaimi, Department of Microbiology, College of Medicine, Al-Iraqia University, Baghdad, Iraq
E-mail Id:
bareq.n.tareq@aliraqia.edu.iq
Orcid Id:
https://orcid.org/0000-0002-5348-1405
How to cite this article:
Al-Rawi M A, Al-Nuaimi B N, Al-mudallal N HA, Al-Rawi M A A. Anti-enzymatic Activity of Alhagi Maurorum Extract and Copper oxide Nanoparticles against Acinetobacter Baumannii Respiratory Infection. J Commun Dis. 2025;57(2):19-31.
Date of Submission: 2025-03-20
Date of Acceptance: 2025-05-25

A B S T R A C T

Background: In respiratory care units (RCU), virulent bacteria have been an enormous burden in respiratory tract infection treatments. Many of these bacteria produce enzymes that are usually associated with virulence, resistance, and pathogenicity. Acinetobacter baumannii is one of the most abundant infections in RCU.

Aim: The present research was conducted for the green synthesis of copper oxide nanoparticles (CuONPs) via *Alhagi maurorum* extract to study anti-enzymatic activity against *Acinetobacter baumannii* isolated from sputum samples.

Methods: Sputum samples isolated and identified by growing on MacConkey agar, blood agar and chocolate agar, and the VITEK-2 compact system. Bacterial enzymatic activity was determined by the agar-well diffusion method. Copper oxide nanoparticles (CuONPs) were prepared using *Alhagi maurorum* plant extract. Characterisation was done by UV-visible spectroscopy, energy dispersive X-ray analysis, Fourier transform infrared (FTIR), X-ray diffraction (XRD), zeta potential analyses and field emission scanning electron microscopy (FESEM). Anti-enzymatic activity of *Alhagi maurorum* extract, CuONPs and *Alhagi maurorum*-CuONPs (AHCuONPs) was determined against *Acinetobacter baumannii*.

Results: The characterizations confirmed the synthesis of AHCuONPs with high purity and crystalline structure. Fourier transform infrared analysis indicated a strong interaction between *Alhagi maurorum* phytochemicals and CuONPs. Zeta potential measurements of +48.15 mV indicated the stability of the nanoparticles. The enzyme inhibition properties of protease-producing Acinetobacter baumannii were highly significant, with a synergistic effect observed for Alhagi maurorum-CuONPs (AHCuONPs) and with CuONPs alone at 20% concentration.

Conclusion: The anti-enzymatic mechanisms of CuONPs and AHCuONPs represent a promising approach to combat the emergence of Acinetobacter baumannii and limit its virulence by protease-enzyme inhibition.

Keywords: Copper Oxide Nanoparticles, *Alhagi Maurorum* Extract, Anti-Enzymatic, *Acinetobacter Baumannii*, Respiratory Tract Infections

Introduction

Virulent bacteria have emerged as an important problem throughout the world for respiratory tract infections.[1,2] The most common bacteria among respiratory care unit (RCU) patients are *Pseudomonas aeruginosa*, *Staphylococcus aureus*, *Acinetobacter baumannii*, and *Klebsiella pneumoniae*. Unfortunately, these bacteria have turned into difficult-to-treat bacteria because of the resistance developed against the standard usage of antibiotics.[3-5] The pathogenicity and antibiotic resistance of many respiratory tract bacteria require the production of various enzymes.[6] β-lactamases, proteases, and lipases are enzymes that mediate the bacterial dissemination and survival within the host.[7] Bacterial proteases play vital functions in cell physiology, replication, and survival. Extracellular proteases are responsible for the destruction of host tissue as well as the degradation of host defenceproteins including immunoglobulin A (IgA).[8] This has made the need for finding new ways to fight infection more important, including the exploration of new approaches to overcome the severity of many respiratory tract pathogens.[9,10]

Metal oxide nanoparticles (NPs), including copper oxide nanoparticles (CuONPs), represent a promising class of nanomaterials in fighting against bacterial attacks via multiple mechanisms such as reactive oxygen species (ROS) generation, disruption of microbial membranes, and interference with the action of some important enzymes critical for its survival.[11] Some metal oxide nanoparticles present properties involve high biocompatibility and a great surface area available for interaction with biotic materials.[12]

One such field that has a very growing area of interest is the green synthesis of nanoparticles through the use of plant extracts, which have a much less ecological and budgetary cost than other classical chemical approaches.[13] Plants continue to be a significant source of several chemicals that support better human health and potential raw material for nanoparticle synthesis. One promising plant is *Alhagi maurorum* due to its presence of antimicrobial and antioxidant compounds.[14]

Alhagi maurorum is a member of the Fabaceae family and grows widely in sandy soils. The plant blooms in July, and May and might reach a length of two meter.[15] *Alhagi maurorum* demonstrated many preventative qualities, particularly their potent antibacterial and antioxidant effects, as well as their raw extracts and chemical constituents, have been the subject of much researches.[16]

Research has shown that nanoparticles may interfere with the action of many enzymes, therefore reducing the pathogenicity of various bacteria by inhibition of some virulence factors.[17] The present study investigated anti-enzymatic activity of CuONPs synthesisedusing *Alhagi maurorum* extract against Acinetobacter baumannii isolated and identified from sputum samples of patients in respiratory care units (RCUs). This approach could help find sustainable and effective ways to treat and control infections caused by antibiotic-resistant pathogens.

Materials and Methods

Collection of sputum samples

The present study was conducted in the period between November 2023 and July 2024. One hundred (100) sputum samples were collected from (38) females, (53) males and (9) children's patients who were admitted to the RCU in Al-Yarmouk Teaching Hospital and Neurosurgery Teaching Hospital. Samples were aseptically collected in sterile vials and transported to the laboratory. The study received ethical clearance from the Ethical Committee of Al-Iraqia University/ College of Medicine/Microbiology Department.

Isolation of bacteria and determination of antibiotic resistance

The sputum samples were cultured on blood, chocolate, and MacConkey agars to isolate the bacterial pathogens of the respiratory tract. Subculturing was performed onto freshly prepared media to purify the mixed cultures. The isolates were identified using standard microbiological techniques, such as Gram staining and biochemical tests (urease and Simmons citrate)[18] The antibiotic resistance and diagnostic bacteria of the isolates were determined by using the VITK-2 system following the manufacturer's instructions.

Detection of protease-producing bacterial isolates

The protease enzyme activity was determined using skim milk agar medium. For preparation of skim milk agar, 51.5 grams of nutrient agar weresuspended in 1 litre

of distilled water and boiled until complete dissolution. Sterilisation was done by autoclaving the medium at 121°C for 15 minutes. It was allowed to cool to 45°C, and 5 mL skim milk was added and then dispensed into sterile Petri dishes.[19] Protease production was detected in the bacterial isolates by measuring the clearance zone diameter in skim milk agar. After preparing the milk skim agar, a cork borer with a diameter of 0.6 mm was used to make four wells in each Petri dish. The bacterial suspension was adjusted with McFarland solution 1.5 x 10^8 and dispensed into each well to detect which isolates produced protease. The bacterial suspension that grew on nutrient broth before one day of incubation at 37°C was diluted with sterile normal saline and compared with the McFarland Standard (1.5 x 10^8).[20]

Collection and preparation of *Alhagi maurorum* plant extract

Fresh *Alhagi maurorum* plants were collected from their natural habitat in Abo-Gareeb, Baghdad. The plant material

ISSN: 0019-5138
DOI: https://doi.org/10.24321/0019.5138.202533

was washed with distilled water, air-dried, and ground into a fine powder to extract compound.[13] The air-dried ground *Alhagi maurorum* plant material, weighted 100 grams for each sample, was extracted with the aqueous methanol (methanol: water, 80 % v/v), (500 mL) solvent for 8 hours under Soxhlet on a water bath in separate experiments.[21] The extracts were concentrated and freed of solvent under reduced pressure at 45°C using a rotary evaporator. The dried crude concentrated extracts were weighed to calculate the yield and stored in a refrigerator at 4°C until used.

Synthesis of Copper Nanoparticles

Polyvinyl alcohol (PVA)and vitamin C (1%) were added to freshly prepared 0.2 M copper nitrate solution in a ratio of 1:1:3, respectively. Accompanied with constant stirring, the solution was heated for 4 hours at 55°C until a colour change was observed with some modification. The fully reduced solution was centrifuged for 15 minutes at room temperature (5000 rpm), washed, and stored at 4°C until further use.[22-24]

Preparation of *Alhagi maurorum*-Copper Oxide Nanoparticles

To 200 mL of distilled water, the powdered plant materials were added and heated at 60°C for 30 minutes. The resultant heated mixture was filtered by using Whatman No. 1 filter paper. The obtained filtrate was stored at 4°C and used later for the synthesis of nanoparticles.[17] A concentration of 0.1 M aqueous solution of copper sulphate ($CuSO_4$) was prepared. *Alhagi maurorum* extract was added dropwise to copper sulphate (($CuSO_4$)) solution under stirring conditions. The reaction mixture was kept at 70°C for 2 hours; due to time, colouring changes indicated the development of *Alhagi maurorum*-copper oxide nanoparticles (AHCuONPs). Centrifugation of the solution was performed at 10,000 rpm for 20 minutes, followed by washing with distilled water and ethanol and drying at 60°C for 12 hours for further characterisation.[12]

Characterisation of *Alhagi maurorum*-Copper Oxide Nanoparticles

The synthesised nanoparticles were characterised using UV-vis spectroscopy analysis, energy dispersive X-ray analysis, Fourier transform infrared (FTIR), X-ray diffraction (XRD) analysis, zeta potential analyses, and field emission scanning electron microscopy (FESEM).

Determination of anti-enzymatic activity

The determination of anti-enzymatic activity of the nanoparticles (CuONPs), Alhagi maurorum-CuONPs(AHCuONPs), and *Alhagi maurorum* extract was done using the agar well-diffusion method. *Acinetobacter baumannii* bacterial cultures were incubated with three different concentrations, 10%, 20%, and 40%, of tested solutions.[16] An amount of the respective tested solution was added into a bacterial suspension in a sterilised container; subsequently, an aliquot of 0.1 ml of that mixture was introduced into separated wells on nutrient agar. The positive control had 0.1 ml of bacterial suspension adjusted to McFarland standard without any addition, and a negative control constituted 0.1 ml of normal saline. One well was treated with *Alhagi maurorum* extract mixed with the bacterial suspension, which was adjusted to the McFarland standard, and in another well, maurorum-CuONPs mixture with bacterial suspension adjusted to the McFarland standard was added. A separate well was prepared with 0.1 ml of the nanoparticles, CuONPs, mixed with bacterial suspension, also adjusted to the McFarland standard (to measure the concentration of bacteria). The nutrient agar plates were incubated at 37°C for 24 hours to allow bacterial growth and evaluate the anti-enzymatic activity of the test solutions.

Statistical analysis

Triplicate sets of all experiments were performed, and the data obtained was subjected to a statistical package (IBM SPSS, Chicago, IL, USA; version 29). Values obtained were expressed as mean ± standard error of mean (SEM). For testing significant differences in quantitative data, a Student's T-test comparing two independent means or more than two independent means through ANOVA was employed. A P-value of ≤ 0.05 was considered statistically significant.

Results

Bacterial isolation, identification and antibiotic resistance

One hundred sputum samples (100) were cultivated on blood agar, MacConkey agar, and chocolate agar to identify the bacterial species. The isolates have undergone plenty of biochemical tests, including the triple sugar iron (TSI) assay, urea hydrolysis, and Simmon's citrate. The results of biochemical tests were demonstrated in table 1. Gram-stained bacterial smears examined under a microscope to show the variations in cell shapes. Forty-three of the sputum samples (43/100) showed no signs of bacterial development, while fifty-seven samples (57/100) have presented growing bacterial colonies. Results revealed that *Acinetobacter baumannii* and *Klebsiella pneumoniae* were the most isolated bacteria in the RCU sputum samples, with 34 (34%) and 28 (28%) isolates, respectively (table 2).

Acinetobacter spp. presented in 47.4% (27/57) of the positive isolates of RCU sputum samples (figure 1). *Acinetobacter baumannii* detected in (7/57). Other bacterial isolates include eighteen (18/57) isolates of Klebsiella species, one (1/57) isolate of Proteus mirabilis, one (1/57)

ISSN: 0019-5138
DOI: https://doi.org/10.24321/0019.5138.202533

isolate of *Staphylococcus aureus*, one isolate (1/57) of *Pseudomonas aeruginosa*, and three (3/57) samples of normal flora. The VITEK-2 system was used to further validate identification. All samples were found resistant to amikacin, gentamicin, tobramycin, ciprofloxacin, pefloxacin, minocycline, colistin, rifampicin, trimethoprim, ceftazidime, cefepime, aztreonam, imipenem, and meropenem.

Table 1.Biochemical tests of gram-negative bacterial isolates

Bacterial isolates	Gram stain	Citrate test	Lactose fermentation	Indole test (peptone water)	Triple sugar iron (TSI)	Urease test	Oxidase test	Catalase test
Klebsiella pneumonia	-	+	+	-	A/A+-	+	_	+
Acinetobacter baumannii	-	+	+	-	k/k	-	-	+
Proteus mirabilis	-	+	-	-	K/A++	+	-	+
Pseudomonas aeruginosa	-	+	-	-	K\K -	-	+	+

Table 2.Percentage occurrence of bacterial isolates from sputum samples

Bacterial isolate	Frequency of occurrence	Percentage occurrence
Acinetobacter species	27	47.4
Acinetobacter baumannii	7	12.3
Klebsiella species	18	14.0
Klebsiella pneumonia	10	17.4
Proteus marinus	1	1.8
Staphylococcus aureus	1	1.8
Normal flora	3	5.3
Total	57	100.0

Figure 1.Acinetobacter on MacConkey agar

ISSN: 0019-5138
DOI: https://doi.org/10.24321/0019.5138.202533

Production of protease enzyme by *Acinetobacter baumannii*

Acinetobacter baumannii was selected from the isolated species to reveal the enzymatic activity (protease production). The ability of this bacteria to produce enzyme was assessed using a protease enzyme assay for each of *Acinetobacter baumannii* isolates. Further analysis revealed that the protease enzyme was produced in four (4/7) isolates. Clear zones surrounding bacterial colonies were observed confirming protease production (figure 2).

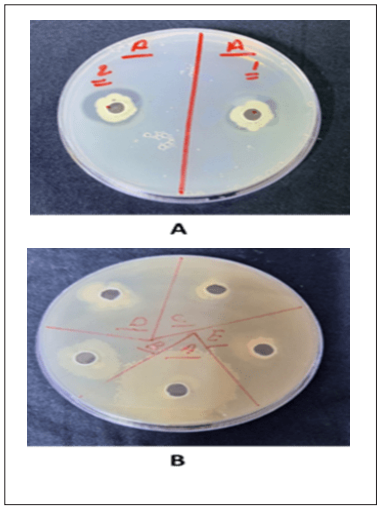

Figure 2.Protease production by *Acinetobacter baumannii*

Characterisationof *Alhagi maurorum* plant extract and copper oxide nanoparticles

UV-visible spectroscopy (UV-Vis) analysis of nanoparticles

UV-Vis's absorption spectra were performed on various tested solutions, including the nanoparticles $CuSO_4$, CuONPs, *Alhagi maurorum* extract, and *Alhagi maurorum*-CuONPs. In the UV-Vis spectrum of $CuSO_4$, a very clear absorption peak could be viewed due to typical d-d electronic transitions of Cu^{2+}ions in solution (Figure 3A). The other solution, CuONPs, exhibited an SPR peak in the visible region due to the formation of nanoparticles and the collective oscillation of conduction band electrons (Figure 3B). *Alhagi maurorum* extract demonstrated specific absorbance peaks associated with its bioactive compounds, including phenolics and flavonoids, which are likely involved in the bio-reduction and capping of nanoparticles (Figure 3C). The spectrum of *Alhagi maurorum*- stabilised CuONPs combines features from both the CuONPs and the *Alhagi maurorum* extract, with a shift in the SPR peak compared to CuONPs alone (Figure 3D). This shift suggests successful stabilisationand functionalisationof CuONPs by the extract, potentially due to the interaction of phytochemicals with the nanoparticle surface. These findings confirm the synthesis and stabilisationof CuONPs by *Alhagi maurorum* extract, highlighting its role as both a reducing and capping agent in the green synthesis of nanoparticles.

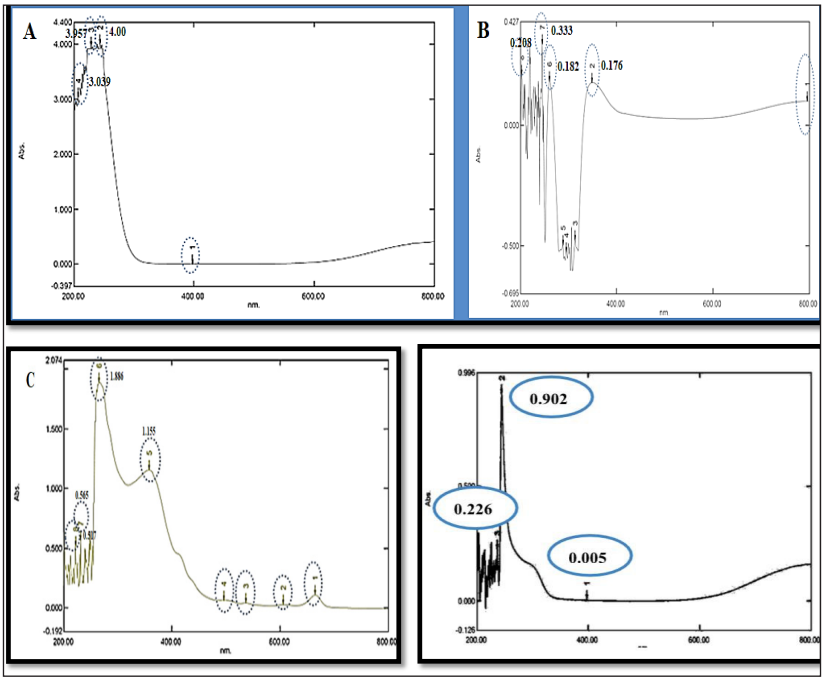

Figure 3.Ultraviolet-visible spectroscopy of test solutions. (A) resemblesCuSO4; (B) resembles Copper oxide nanoparticles (CuONPs); (C) resembles *Alhagi maurorum* extract; and (D) resembles *Alhagi maurorum* extract -CuONPs (AHCuONPs)

ISSN: 0019-5138
DOI: https://doi.org/10.24321/0019.5138.202533

Energy dispersive X-ray analysis of nanoparticles: elemental composition

The energy-dispersive X-ray spectrum of *Alhagi maurorum*-stabilized CuONPs confirms the elemental composition of the stabilised nanoparticles, with prominent peaks corresponding to copper (Cu) and oxygen (O), indicative of the successful formation of copper oxide (CuO) (Figure 4). The significant Cu peak arises from the metallic core of the nanoparticles, while the O peak suggests the presence of oxide species, affirming the oxide nature of the nanoparticles. Additionally, weaker signals for other elements such as carbon (C) may be attributed to organic phytochemicals from the *Alhagi maurorum* extract used as a reducing and capping agent during the synthesis process. The absence of peaks for impurities highlights the high purity of the synthesised CuONPs. These results corroborate the role of *Alhagi maurorum* extract in the eco-friendly synthesis of CuONPs, where its bioactive components facilitate the reduction of copper ions and stabilise the resulting nanoparticles. Figure 4 was accomplished with an insert (Table 1) that delineates the atomic percentages of elements in the synthesised *Alhagi maurorum* extract, CuONPs, and *Alhagi maurorum*-CuONPs (AHCuONPs).

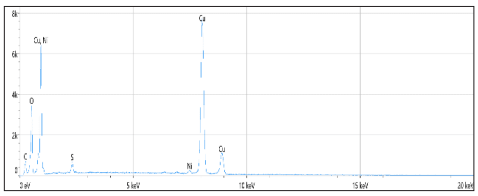

Figure 4.Energy dispersive X-ray (EDX) spectrum of *Alhagi maurorum* extract-copper oxide nanoparticles (CuONPs)

The elemental composition analysis highlights the distinct profiles of Alhagi maurorum, CuONPs, and *Alhagi maurorum*-CuONPs (AHCuONPs). *Alhagi maurorum* extract contains high levels of carbon (62.1%) and oxygen (31.2%), with minor amounts of sodium, calcium, and magnesium, indicating an organic and mineral-rich nature. In CuONPs, oxygen (50.1%) and copper (25.1%) dominate, with carbon (24.8%) likely from synthesis residues. The composite, AH-CuONPs, exhibits a balanced elemental profile of oxygen (44.6%), carbon (22%), and copper (31.1%), along with trace amounts of sulphur (1.4%) and nickel (0.5%). This suggests successful integration of CuONPs into the *Alhagi maurorum* matrix, resulting in a more complex elemental profile compared to the individual components (table 3).

Functional group determination: Fourier transforms infrared analysis (FTIR)

FTIR examination of the samples was performed in the range of 400-4000 cm^{-1}. FTIR analysis was used to detect the functional groups potentially responsible for the reduction of copper nanoparticles from *Alhagi maurorum* extract and their stabilisation. Results of the variations in the chemical bonds characteristic of the peaks responsible for the stretching vibrations of the –OH groups were referred to the phenolic compounds present in the FTIR spectra of the plant extract (3370.25 cm-1) and copper nanoparticles from *Alhagi maurorum* extract at (3415.93 cm-1), but the disappearance of other peaks when examining the FTIR of the same sample, which are (1037.10, 1068.36, 1203.68, 1238.0, 1364.03 and 1512.19) cm-1 indicate the extension of C-N stretch, C-H rock, N-O symmetric stretch, and the disappearance of the peaks from 753.24- 835.19 cm-1 (aromatic cyclic compounds). The peaks at 526.50 and 509.21 cm-1 appeared for copper nanoparticles from *Alhagi maurorum* extract, and copper nanoparticles, respectively, were indicated to copper presented. indicating successful interaction between the extract's bioactive compounds and the nanoparticle matrix. Specifically, the broad O–H band is slightly shifted, suggesting stabilisation of nanoparticles through hydrogen bonding or other surface interactions. Peaks around 1600 cm^{-1} remain prominent, confirming the retention of aromatic compounds (figure 5).

X-ray diffraction (XRD) analysis of nanoparticles: crystalline structure

The diffraction peaks in both CuONPs and *Alhagi maurorum*-stabilised CuONPs patterns revealed valuable information about the crystalline structure of the synthesised nanoparticles. The XRD pattern of CuONPs exhibited sharp and well-defined peaks at specific 2θ values, corresponding to characteristic planes of copper oxide, CuO (Figure 6A). These peaks confirm the formation of highly crystalline monoclinic CuO indexed by the Joint Committee on Powder Diffraction Standards (JCPDS). In the case of *Alhagi maurorum*- stabilised CuONPs, the XRD pattern retains the characteristic peaks of CuO observed in figure 6A, showing that the crystallinity of the nanoparticles is preserved after stabilisation. However, some extra peaks of lower intensity were observed, which may be due to the amorphous organic components of *Alhagi maurorum* extract adsorbed on the nanoparticle surface (figure 6B). The absence of any

Table 3.Elemental composition of tested solutions

Tested Solutions	Elements (Atomic %)							
	C	Na	Ca	Mg	O	S	NI	Cu
Alhagi maurorum	62.1	3.8	1.9	0.94	31.2	-	-	-
CuONPs nanoparticles	24.8	-	-	-	50.1	-	-	25.1
Alhagi maurorum-CuONPs	22	-	-	-	44.6	1.4	0.5	31.1

ISSN: 0019-5138
DOI: https://doi.org/10.24321/0019.5138.202533

extraneous peaks in both spectra confirms the purity of the samples, which further proves that no impurities or other phases were introduced during the synthesis process. These results substantiate the successful synthesis of crystalline CuONPs and their stabilisationby *Alhagi maurorum* extract. The consistent crystallinity and absence of impurity phases further validate the efficiency of *Alhagi maurorum* as a bio-template for eco-friendly nanoparticle synthesis.

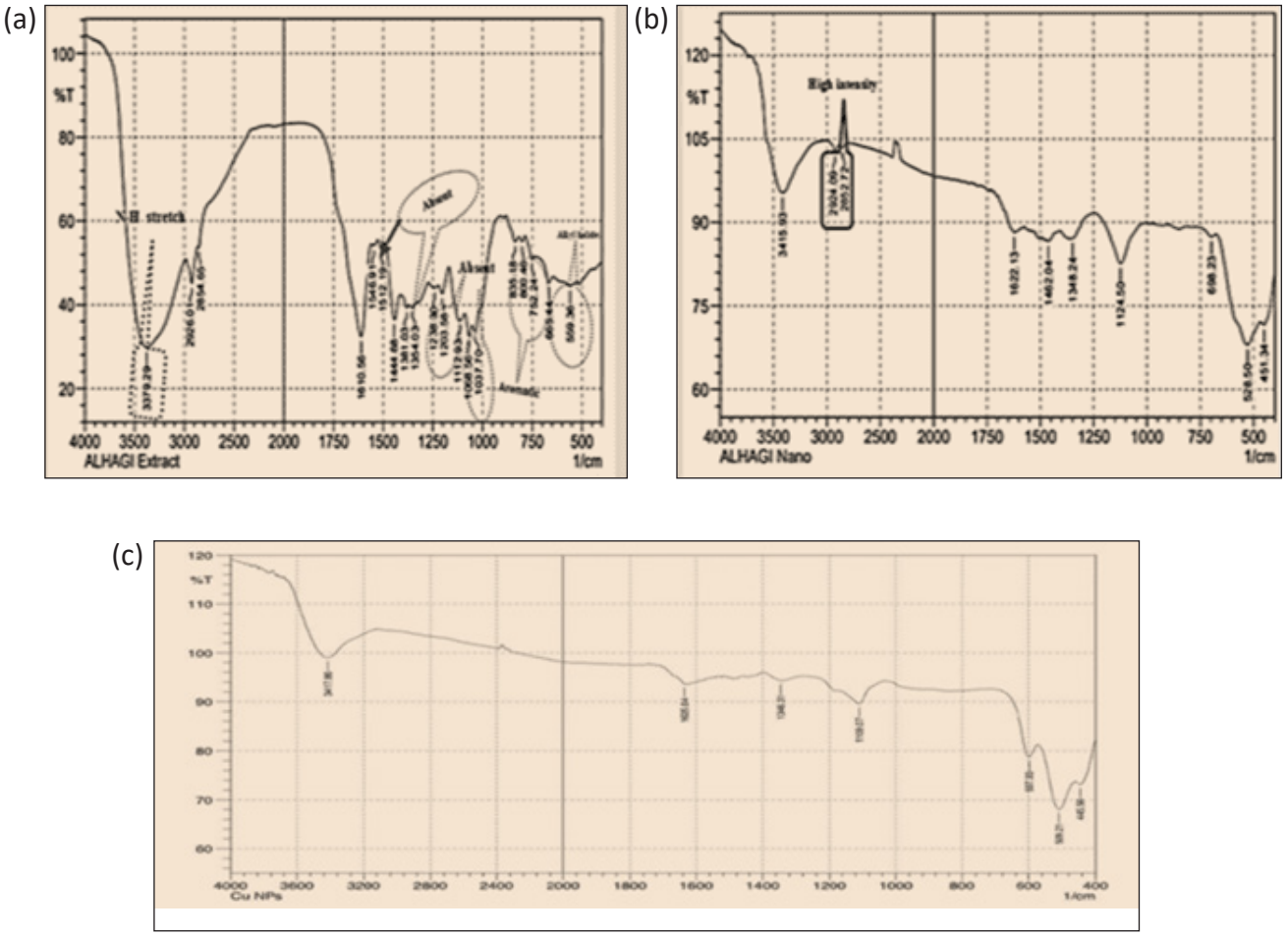

Figure 5.FTIR analysis of *Alhagi maurorum* extract is showedshown in (A), and *Alhagi maurorum* extract-copper oxide nanoparticles are showedshown in (B),and copper oxide nanoparticles showed nanoparticles are shown in (C)

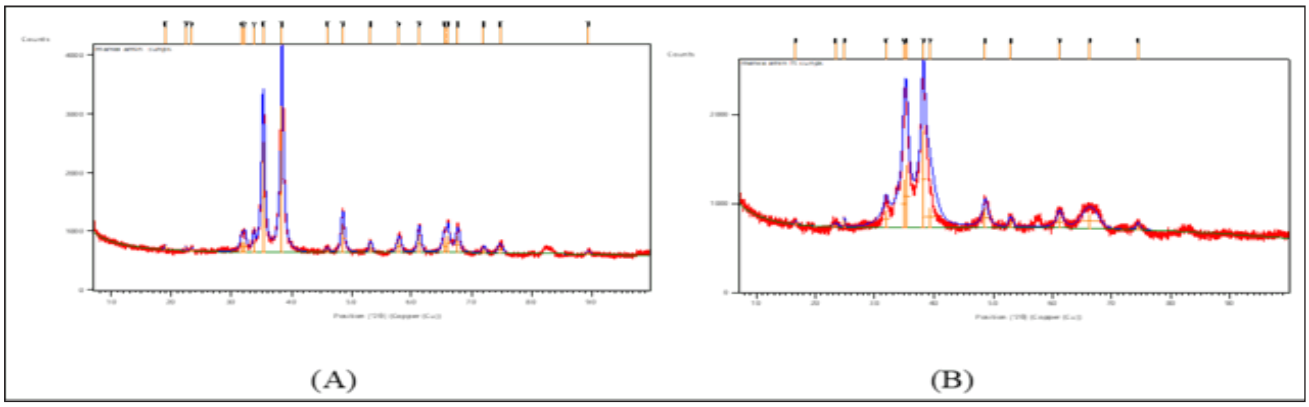

Figure 6.X-ray diffraction (XRD) analysis of test solutions. A: Copper oxide nanoparticles (CuONPs); B: *Alhagi maurorum* extract-CuONPs

ISSN: 0019-5138
DOI: https://doi.org/10.24321/0019.5138.202533

Zeta potential analysis of nanoparticles: Surface charge and stability

The zeta potential of the synthesised nanoparticles shows that the zeta potential of *Alhagi maurorum*-CuONPs, measured at +48.15 mV, indicates good stability due to strong electrostatic repulsion (figure 7A). The zeta potential of CuONPs, measured at +59.82 mV, reflects a higher degree of stability than *Alhagi maurorum*-CuONPs (figure 7B). The positive zeta potential values suggest that both nanoparticles exhibit significant surface charges, which may enhance colloidal stability in dispersion.

Field Emission Scanning Electron Microscopy (FESEM)

CuONPs samples consist of randomly orientated nano-sized particles with regular smooth spherical shapes. The average size of CuONPs was estimated to be 39.53-64.52 nm. While the images for the AHCuONP samples consist of random nanoparticle-size size particles with regular smooth spherical shapes. The range size of AHCuONPs was (66.06-90.73) nm. The formation of size and shape for the copper nanoparticles and AHCuONPs indicates the interconnection between CuONPsand *Alhagi maurorum* (Figure 8).

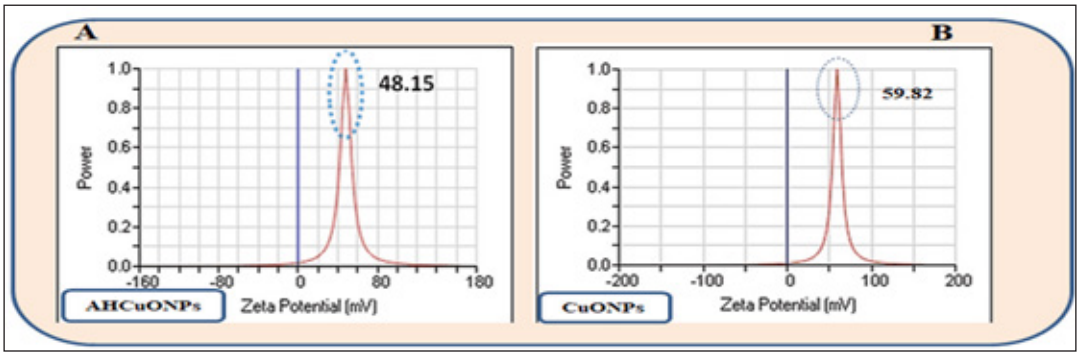

Figure 7.Zeta potential analysis. (A) *Alhagi maurorum*-copper oxide nanoparticles (AHCuONPs) and (B) copper oxide nanoparticles (CuONPs)

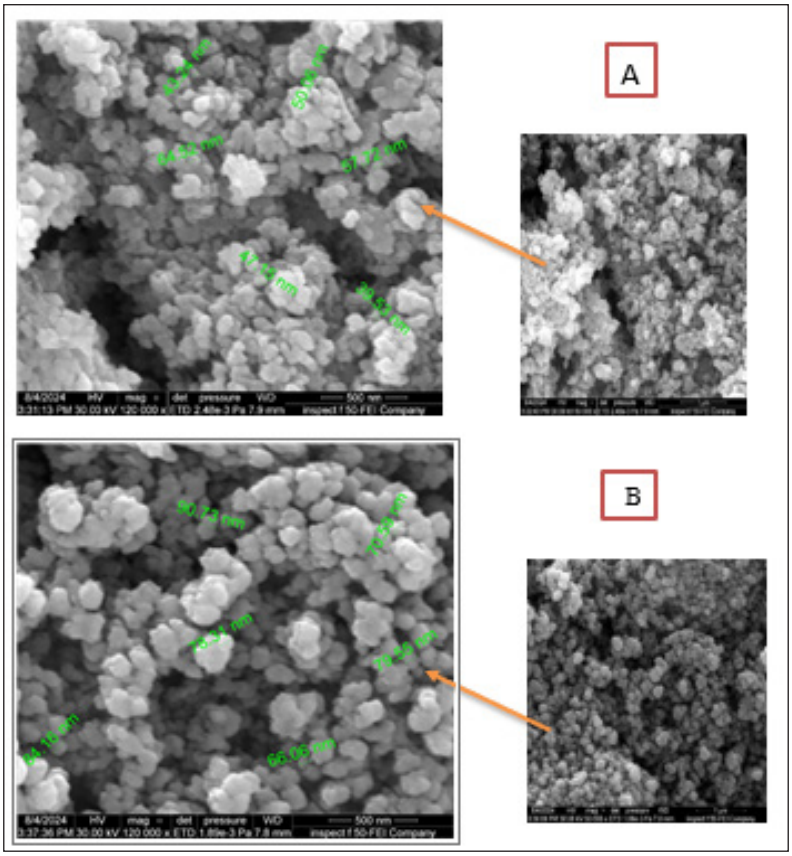

Figure 8.Field Emission Scanning Electron Microscopy (FESEM) images: (A) represent CUONPs; (B) represents AHCuONPs

ISSN: 0019-5138
DOI: https://doi.org/10.24321/0019.5138.202533

Inhibition of enzymatic activity against *Acinetobacter baumannii*

The effect of *Alhagi maurorum* extract, CuONPs, and a combination of *Alhagi maurorum*-CuONPs against protease-producing *Acinetobacter baumannii* wasconducted. Varying concentrations (10%, 20%, and 40%) of CuONPs, *Alhagi maurorum*-CuONPs, and *Alhagi maurorum* extract on three isolates of *Acinetobacter baumannii* (*Acinetobacter* 1, 2, 3, and 4) with controls included for comparison. The results demonstrated variations in anti-enzymatic efficacy depending on the treatment type and concentration (figure 9).

Dealing with the first isolate, adding CuONPs (10%, 20%, and 40%) to the control resulted in a concentration-dependent effect, with higher concentrations showing more pronounced changes (Figure 9 IA). *Alhagi maurorum*-CuONPs exhibited enhanced effects compared to CuONPs, suggesting increased efficacy likely due to synergistic interactions between *Alhagi maurorum* and CuONPs (Figure 9 IB). Similarly, *Alhagi maurorum* extract demonstrated a concentration-dependent trend, though the effects were less pronounced than those observed with *Alhagi maurorum*-CuONPs (Figure 9, IC). CuONPs showed a consistent concentration-dependent response in the second *Acinetobacter baumannii* isolate, with 40% demonstrating the strongest effect (figure 9, IIA). *Alhagi maurorum*-CuONPs were more effective than CuONPs alone, confirming the potential enhancement from *Alhagi maurorum* (Figure 9, IIB). *Alhagi maurorum* extract produced a moderate response, with increasing concentrations resulting in stronger effects (Figure 9, IIIC). In *Acinetobacter baumannii* isolate no. 3, the CuONPs showed similar behaviour to previous isolates, with higher concentrations leading to more noticeable changes (Figure 9, IIIA). *Alhagi maurorum*-CuONPs again outperformed CuONPs, indicating their superior impact (Figure 9, IIIB). *Alhagi maurorum* extract exhibited a steady concentration-dependent effect, though slightly less impactful than the CuONPs and *Alhagi maurorum*-CuONPs (Figure 9, IIIC). CuONPs produced a clear concentration-dependent response in Acinetobacter isolate no. 4 (Figure 9, IVA). *Alhagi maurorum*-CuONPs demonstrated the highest effectiveness among all tested nanoparticles, showing the strongest impact at 40% (Figure 9, IVB). *Alhagi maurorum* extract NPs followed a similar trend, though their impact was less pronounced than the composite CuONPs formulations. Across all Acinetobacter isolates (1-4), the combination of *Alhagi maurorum* and CuONPs consistently showed enhanced efficacy over CuONPs or *Alhagi maurorum* extract alone. This suggests a synergistic effect between *Alhagi maurorum* and CuONPs, making them a promising option for antimicrobial applications. The effectiveness of all treatments increased at 20% concentration of CuONPs and *Alhagi maurorum*-CuONPs exhibiting the strongest anti-enzymatic activity against protease (table 4 and figure 10).

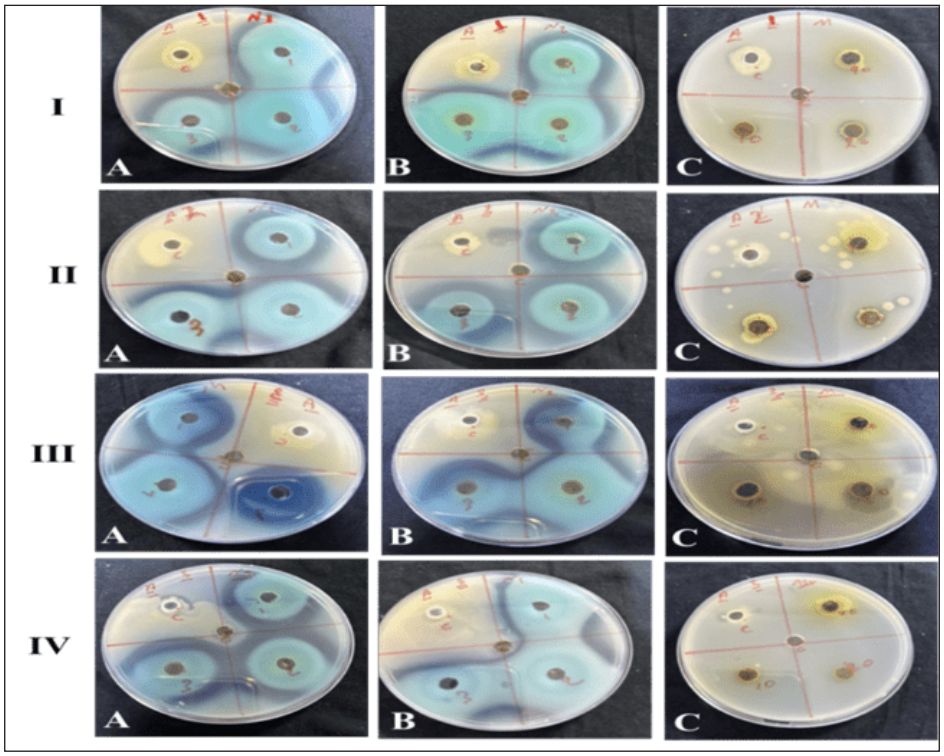

Figure 9.Anti-enzymatic activity of *Alhagi maurorum* extract-copper oxide nanoparticles against isolates of *Acinetobacter* species

ISSN: 0019-5138
DOI: https://doi.org/10.24321/0019.5138.202533

Table 4.The inhibition zones (mm) of *Acinetobacter baumannii* after treatment by *Alhagi maurorum* extract, CuONPs, and a combination of *Alhagi maurorum*-CuONPs

Material & Concentration	Acinetobacter baumanni	P value compared to Control+Bacteria
Cu 10%	39.5±3.5 (35-47)	0.0001#
Cu 20%	44.3±4.7 (38-53)	0.0001#
Cu 40%	37.3±5.4 (28-44)	0.0001#
Cu+M 10%	36.3±4.0 (28-43)	0.0001#
Cu+M 20%	41.5±3.3 (37-48)	0.0001#
Cu+M 40%	36.8±3.7 (32-44)	0.0001#
M only 10%	10.1±3.3 (6-17)	0.969
M only 20%	10.8±1.7 (9-14)	0.996
M only 40%	17.5±3.6 (11-22)	0.013#
Control+Bacteria	11.7±3.3 (7-16)	-
Distilled water	0.0±	-

#Significant difference between two independent means using Students-t-test at 0.05 level.

^Significant difference among more than two independent means using ANOVA-test at 0.05 level.

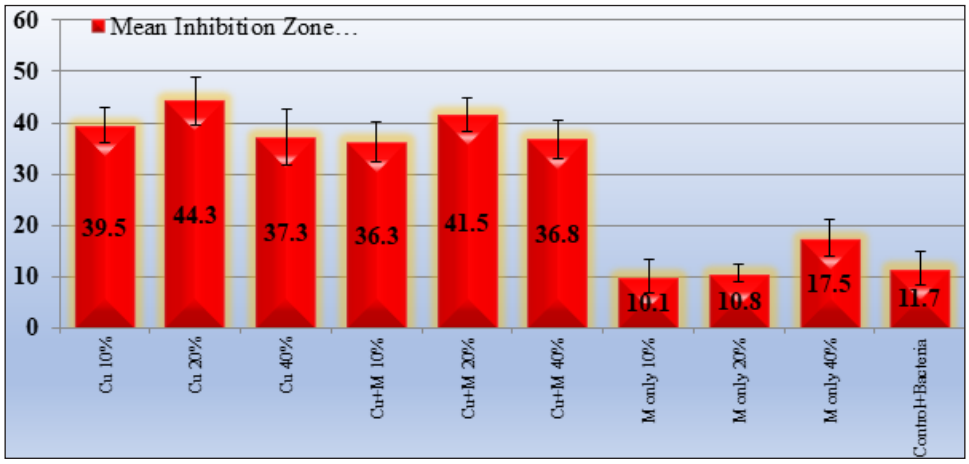

Figure 10.Anti-enzymatic activity of tested solutions against protease-producing *Acinetobacter baumannii*

Discussion

The increasing prevalence of multi-drug resistant (MDR) bacterial strains, especially in hospital settings, is a key challenge in managing respiratory tract infections. Various enzymes, including proteases, lipases, and β-lactamases, are associated with the virulence, resistance, and pathogenicity of the microorganisms. Protease-producing Acinetobacter, particularly *Acinetobacter baumannii*, is a significant concern in respiratory tract infections. This pathogen is known for its antibiotic resistance and virulence factors, which make it particularly dangerous in healthcare settings. Bacterial proteases play a crucial role in respiratory tract infections by aiding bacteria in colonising and invading host tissues.[25,26]

In the light of these findings, this study addresses an urgent need for alternative strategies by investigating the anti-enzymatic properties of the *Alhagi maurorum*-mediated copper oxide nanoparticles against one of the most important bacterial pathogens isolated from sputum samples of RCU patients which is Acinetobacter spp. The findings identified a synergistic interplay in the phytochemicals of Alhagi maurorum, together with the antimicrobial potential of CuONPs, which present encouraging perspectives in counteracting MDR bacterial infections.

The UV-Vis absorption spectra confirmed the successful synthesis of CuONPs and their stabilisation by *Alhagi maurorum* extract. The observed surface plasmon resonance

ISSN: 0019-5138
DOI: https://doi.org/10.24321/0019.5138.202533

(SPR) peak in CuONPs aligns with earlier reports by Banerjee et al. (2014), who demonstrated the characteristic SPR peak in green- synthesised CuONPs. However, the shift in the SPR peak for *Alhagi maurorum*-CuONPs compared to CuONPs alone highlights the extract's role in nanoparticle functionalisation, as also noted by Ali et al. (2020) in their study on plant-extract-mediated nanoparticle synthesis. Unlike prior studies using synthetic stabilisers, the approach in the present study underscores the dual role of *A. maurorum* as a reducing and capping agent, demonstrating the potential for eco-friendly nanoparticle synthesis.[27,28]

Energy dispersive X-ray analysis (EDX) findings revealed the elemental composition of *A. maurorum*-CuONPs, confirming the presence of copper and oxygen, along with trace organic residues from the extract. These findings are consistent with earlier work by Singh et al. (2016), who reported similar elemental profiles in biologically synthesised CuONPs.[29] Notably, the absence of impurities in the samples underscores the purity of the synthesised nanoparticles, a significant improvement over previous methods that often require post-synthesis purification steps.[30]

The FTIR spectra revealed functional groups in the *Alhagi maurorum* plant extract and their interaction with CuONPs. The observed O–H stretching and C=C aromatic peaks are comparable to findings by Kumar et al. (2021), who identified similar functional groups in plant-extract-mediated nanoparticle synthesis.[31] The shifts in peak positions in *A. maurorum*-CuONPs confirm successful stabilisation, consistent with observations by Sharma et al. (2019). This interaction highlights the potential of *A. maurorum* phytochemicals in nanoparticle functionalisation.[32] Researchers rely on a powerful and popular analytical tool, infrared (IR) spectroscopy, when studying the biosynthesis of copper nanoparticles and the structure of copper nanoparticles alone, which depends on the vibrations of the atoms of the molecule. It is possible to qualitatively identify the types of bonds in the sample by comparing the energy of each absorption peak with the vibration frequency of the molecular component. The efficiency and accuracy of IR spectroscopy have been greatly enhanced by the advent of Fourier transform infrared (FTIR) spectroscopy, which has significantly reduced data acquisition times.[33]

The XRD patterns confirmed the monoclinic crystalline structure of CuONPs, with additional amorphous peaks attributed to organic components from *A. maurorum*. Similar crystallinity was reported by Das et al. (2018) for biosynthesised CuONPs.[34] However, the findings in the present study uniquely demonstrate the retention of crystallinity post- stabilisation, emphasinsingthe extract's efficiency as a bio-template. The zeta potential measurements indicated strong stability of *A. maurorum*-CuONPs (+48.15 mV) and CuONPs (+59.82 mV). These values are consistent with earlier studies, such as those by Pandey et al. (2020), which reported high zeta potentials in green-synthesised nanoparticles. Meanwhile, *A. maurorum*-CuONPs showed slightly lower stability than CuONPs, the stability remains sufficient for practical applications, indicating the extract's effective capping ability.[35]

Production of protease was eminently high in a few isolates of *Acinetobacter baumannii*, which once again upholds its relationship with bacterial adaptability and virulence. Previous findings suggest that protease production is strain-specific, which may correlate with the isolates' pathogenicity or environmental adaptability. The present findings revealed that *Acinetobacter* strains possess the capacity for extracellular protease secretion, with potential implications for their pathogenicity and environmental roles.

The significant inhibition of enzymatic activity by CuONPs and AHCuONPs highlights their dual role in antimicrobial action: direct bacterial killing and suppression of virulence factors. This anti-enzymatic activity is particularly relevant in the context of MDR pathogens, where targeting non-essential but virulence-associated enzymes can reduce bacterial fitness and resistance. The observed synergistic effects between *Alhagi maurorum* extract and CuONPs in inhibiting enzymatic activity align with findings by Chong & Shimoda (2020) and Liu et al., 2021), emphasising the potential of nanoparticle-based therapies to disrupt bacterial metabolic pathways.[8,12]

Comparative efficacy and clinical implications

The comparative analysis of CuONPs, the *Alhagi maurorum* extract, and AHCuONPs revealed that the nanoparticles CuONPs (20%) exhibited superior anti-enzymatic properties. This enhancement likely stems from the interaction between CuONPs and *Alhagi maurorum* phytochemicals, which amplify oxidative stress and disrupt bacterial enzymatic systems. Similar synergistic interactions have been reported in studies involving plant-mediated nanoparticle synthesis.[14] The clinical implications of these findings are substantial. AH-CuONPs offer a dual-action approach by directly targeting bacterial viability and virulence factors. This strategy not only reduces bacterial loads but also diminishes the likelihood of resistance development. Moreover, the green synthesis method revealed a good biocompatibility, making AHCuONPs suitable for potential therapeutic applications in respiratory infections and beyond in addition to CuONPs alone.

Limitations and future directions

While the present study provides compelling evidence for the efficacy of AHCuONPs, several limitations warrant

ISSN: 0019-5138
DOI: https://doi.org/10.24321/0019.5138.202533

consideration. The molecular mechanisms underlying the observed anti-enzymatic effects require further investigation. Additionally, *in vivo* studies are essential to evaluate the biocompatibility, safety, and therapeutic potential of AHCuONPs. Future research should also explore the scalability of the green synthesis method and its applicability to other pathogens and enzymatic targets.[36]

Conclusion

The current study focused on the anti-enzymatic activity of each of *Alhagi maurorum* plant extract, the nanoparticles CuNOPS and *Alhagi maurorum*-copper oxide nanoparticles (AHCuONPs) against protease-producing *Acinetobacter baumannii*. The current treatments bear excellent anti-enzymatic activities against *Acinetobacter baumannii* isolated from respiratory care unit patients' sputum. The nanoparticles of CuONPs alone at 20% concentration presented the highest anti-enzymatic activity. The combination of CuONPs with phytochemicals derived from *Alhagi maurorum* expresses an augmented action on microorganisms via hindering virulence factors, including protease enzymes. Future investigations should be directed toward the exact molecular mechanism elucidation for the improved anti-enzymatic properties. Besides, *in vivo* studies are also important in determining their safety, biocompatibility, and therapeutic potential.

Conflict of Interest: None

Source of Funding: None

Authors Contribution: Conceptualization, investigation by MAA. Conceptualization and writing original draft by BNA. Reviewing and supervision by NHAA. Methodology, validation and resources by MAAA

Declaration of Generative AI and AI-Assisted Technologies in the Writing Process: None

References

1. Al-Aameri DA, Zghair SA, Al-Nuaimi BN, Abdul-Ghani MN, Naman ZT, Fadhil ZJ. Evaluation of Susceptibility of Candida species to Six Antifungal Drugs in Iraqi Specimens. J. Commun. Dis. 2024;56(2):2. [Google Scholar]
2. Al-Aameri DA, Zghair SA, Al-Nuaimi BN, Abdul-Ghani MN, Naman ZT, Fadhil ZJ. Evaluation of Susceptibility of Candida species to Six Antifungal Drugs in Iraqi Specimens. J. Commun. Dis. 2024;56(2):2. [Google Scholar]
3. Nisha R, Soniya P, Ashwani K. Multidrug-resistant bacteria in respiratory infections: challenges and future directions. Front Microbiol. 2021;12:854146. doi: 10.3389/fmicb.2021.854146.
4. Qin S, Xiao W, Zhou C, Pu Q, Deng X, Lan L, Liang H, Song X, Wu M. *Pseudomonas aeruginosa*: pathogenesis, virulence factors, antibiotic resistance, interaction with host, technology advances and emerging therapeutics. Signal transduction and targeted therapy. 2022 Jun 25;7(1):199. [Google Scholar]
5. Sulaymonovich DS, Fayzullaev N, Nazirova R, Ishankulov A, Omidi M, Al-Nuaimi BN, ugli Otabek BK, Ikhtiyorovna KD, Mamatqulov M, Faraji M. Single-Atom Silver-Borophene Hybrid Hydrogels for Electrically-Stimulated Wound Healing: A Multifunctional Antibacterial Platform. Biomaterials Science. 2025. [Google Scholar]
6. Pailhoriès H, Herrmann JL, Velo-Suarez L, Lamoureux C, Beauruelle C, Burgel PR, Héry-Arnaud G. Antibiotic resistance in chronic respiratory diseases: from susceptibility testing to the resistome. European Respiratory Review. 2022 May 25;31(164). [Google Scholar] [Pubmed]
7. Fang LJ, Lin XC, Huang D, Pan TT, Yan XM, Hu WG, Zhu H, Xu Z, Zhu XZ, Lu HJ, Chen GP. 1H NMR-based metabolomics analyses in children with Helicobacter pylori infection and the alteration of serum metabolites after treatment. Microbial Pathogenesis. 2020 Oct 1;147:104292. [Google Scholar]
8. Ingmer H, Brøndsted L. Proteases in bacterial pathogenesis. Research in microbiology. 2009 Nov 1;160(9):704-10. [Google Scholar] [Pubmed]
9. Al-Nuaimi BN, Al-Azzawi RH. Correlation between MicroRNA-155 Expression and Viral Load in Severe COVID-19 Patients. J. Commun. Dis. 2024;56(4):4. [Google Scholar]
10. Al-Nuaimi BN, Abdul-Ghani MN, Al-Asadi AB, Al-Maadhidi JF, Al-Aameri DA, Hadab MA. Efficacy of Sars-Cov-2 Vaccines on Severity of Coronavirus Disease in Iraq. The International Tinnitus Journal. 2024 Mar 28:68-72. [Google Scholar]
11. Smith RJ, Patel KM. Disruption of microbial membranes by CuONPs: a novel approach to combating bacterial infections. RSC Adv. 2024;14(3):123-135.
12. Liu Y, Zhang X, Li X, Wang L, Wang Y, Zhang Y. Surface functionalization of nanoparticles for enhanced biocompatibility and therapeutic efficacy in nanomedicine. J Nanobiotechnology. 2021;19:62. doi: 10.1186/s12951-021-00787-w.
13. Jadoun S, Arif R, Jangid NK, Meena RK. Green synthesis of nanoparticles using plant extracts: A review. Environmental Chemistry Letters. 2021 Feb;19(1):355-74. [Google Scholar]
14. Hassan SHA, Saeed MA, Rahman MM, Bukhari SAS, Khan IA. Antimicrobial and antioxidant activity of *Alhagi maurorum* extract and its potential as a therapeutic agent. Front Pharmacol. 2021;12:655. doi: 10.3389/fphar.2021.655.
15. Ali MS, Mehmood M. Botanical and ecological features of *Alhagi maurorum* (Fabaceae): a leguminous plant

with potential medicinal properties. J Med Plants. 2020;8(2):44-56. doi: 10.1234/jmp.2020.055.

16. Bukhari SAS, Ahmad I, Muhammad A, Sharif M, Khan AL. Antibacterial and antioxidant activity of *Alhagi maurorum* extract: a review on its pharmacological potential. Phytochem Rev. 2021;20:1077-1093. doi: 10.1007/s11101-021-09791-3.
17. Reczyńska K, Marchwica P, Khanal D, Borowik T, Langner M, Pamuła E, Chrzanowski W. Stimuli-sensitive fatty acid-based microparticles for the treatment of lung cancer. Materials Science and Engineering: C. 2020 Jun 1;111:110801. [Google Scholar]
18. Ventola CL. The antibiotic resistance crisis: part 1: causes and threats. Pharmacy and therapeutics. 2015 Apr;40(4):277. [Google Scholar] [Pubmed]
19. Wehr HM, Frank JF, editors. Standard methods for the examination of dairy products. American Public Health Association; 2004 Jun. [Google Scholar]
20. Aryal S. McFarland standards-principle, preparation, uses, limitations. Microbe Notes. URL https:// microbenotes. com/mcfarland-standards/(accessed 6.16. 22). 2021. [Google Scholar]
21. Sultana B, Anwar F, Ashraf M. Effect of extraction solvent/technique on the antioxidant activity of selected medicinal plant extracts. Molecules. 2009 Jun 15;14(6):2167-80. [Google Scholar] [Pubmed]
22. Thakur S, Sharma S, Thakur S, Rai R. Green synthesis of copper nano-particles using Asparagus adscendens roxb. Root and leaf extract and their antimicrobial activities. Int. j. curr. microbiol. appl. sci. 2018 Apr 10;7(4):683-94. [Google Scholar]
23. Sankar R, Manikandan P, Malarvizhi V, Fathima T, Shivashangari KS, Ravikumar V. Green synthesis of colloidal copper oxide nanoparticles using Carica papaya and its application in photocatalytic dye degradation. Spectrochimica Acta Part A: Molecular and Biomolecular Spectroscopy. 2014 Mar 5;121:746-50. [Google Scholar] [Pubmed]
24. Chandraker SK, Lal M, Ghosh MK, Tiwari V, Ghorai TK, Shukla R. Green synthesis of copper nanoparticles using leaf extract of Ageratum houstonianum Mill. and study of their photocatalytic and antibacterial activities. Nano Express. 2020 May 12;1(1):010033. [Google Scholar]
25. Yao Y, Chen Q, Zhou H. Virulence factors and pathogenicity mechanisms of *Acinetobacter baumannii* in respiratory infectious diseases. Antibiotics. 2023 Dec 18;12(12):1749. [Google Scholar] [Pubmed]
26. Russell MW, Kilian M, Mestecky J. Role of IgA1 protease-producing bacteria in SARS-CoV-2 infection and transmission: a hypothesis. Mbio. 2024 Oct 16;15(10):e00833-24. [Google Scholar] [Pubmed]
27. Abbasi T, Anuradha J, Ganaie SU, Abbasi SA. Biomimetic synthesis of nanoparticles using aqueous extracts of plants (botanical species). Journal of Nano Research. 2015;31:138-202. [Google Scholar]
28. Ali M, Khan T, Fatima U, Hameed A. Phytochemical-mediated synthesis of nanoparticles and their antimicrobial applications: A comprehensive review. Environmental Nanotechnology, Monitoring & Management. 2020; 14: 100392-407.
29. Singh P, Kim YJ, Zhang D, Yang DC. Biological synthesis of nanoparticles from plants and microorganisms. Trends in biotechnology. 2016 Jul 1;34(7):588-99. [Google Scholar] [Pubmed]
30. Ahmed S, Ahmad M, Swami BL, Ikram S. Green synthesis of silver nanoparticles using Azadirachta indica aqueous leaf extract. Journal of radiation research and applied sciences. 2016 Jan 1;9(1):1-7. [Google Scholar]
31. Singh J, Kumar V, Kim KH, Rawat M. Biogenic synthesis of copper oxide nanoparticles using plant extract and its prodigious potential for photocatalytic degradation of dyes. Environmental research. 2019 Oct 1;177:108569. [Google Scholar]
32. Sharma D, Kansal R, Kumar A, Applications T. Phytochemical-mediated synthesis of metal nanoparticles and their therapeutic applications. Journal of Molecular Liquids. 2019; 290: 111131-43.
33. Dutta A. Fourier transform infrared spectroscopy. Spectroscopic methods for nanomaterials characterization. 2017 Jan 1:73-93. [Google Scholar]
34. Das RK, Brar SK, Verma M, Surampalli RY. Green synthesis of nanomaterials. Environmental Chemistry Letters. 2014; 12(2): 135–149.
35. Pandey S, Goswami GK, Nanda KK. Green synthesis of nanoparticles: Advances and challenges. Chemical Engineering Journal. 2020; 379: 122435-44.
36. Al-Nuaimi BN, Al-Azzawi RH, Naji RZ. ASSOCIATION OF HUMAN CYTOMEGALOVIRUS WITH HER2 PROTO-ONCOGENE OVEREXPRESSION IN IRAQI BREAST CANCER PATIENTS. Biochemical & Cellular Archives. 2019 Apr 1;19(1). [Google Scholar]

ISSN: 0019-5138
DOI: https://doi.org/10.24321/0019.5138.202533